Mediated interactions and damping effects in superfluid mixtures of Bose and Fermi gases

Dong-Chen Zheng,[1,2] Yu-Xin Liao,[1,2] Wen Lin,[3] and Renyuan Liao[1,2,*]

[1]*Fujian Provincial Key Laboratory for Quantum Manipulation and New Energy Materials, College of Physics and Energy, Fujian Normal University, Fuzhou 350117, China*

[2]*Fujian Provincial Collaborative Innovation Center for Advanced High-Field Superconducting Materials and Engineering, Fuzhou 350117, China*

[3]*College of Physics and Electronic Engineering, Chongqing Normal University, Chongqing 401331, China*

(Received 28 April 2023; revised 26 December 2023; accepted 5 February 2024; published 26 February 2024)

We investigate the homogeneous superfluid mixtures of a Bardeen-Cooper-Schrieffer (BCS) superfluid originating from pairing two-species fermionic atoms and superfluidity stemming from condensation of bosonic atoms. By integrating out the freedoms associated with the BCS superfluid, we derive the fermion-mediated interactions between bosons, which is attractive and can be tuned from long range in the BCS region to short range in the region of Bose-Einstein condensation of molecular dimers. By analyzing the Bogoliubov spectrum and the damping rate of bosonic superfluid, we map out the phase diagram spanned by the boson-fermion mass ratio and the boson-fermion coupling strength, which consists of a phase separation region and two phase-mixing regions with and without Landau damping. The three different phases can coexist at a tricritical point, which moves toward a low boson-fermion mass ratio and a high boson-fermion scattering length as the fermion-fermion interaction strength is tuned up on the BCS side.

DOI: 10.1103/PhysRevA.109.023327

I. INTRODUCTION

Mediated interactions play a crucial role in our understanding of nature. In particle physics, all fundamental interactions are mediated by gauge bosons [1]. In condensed-matter physics, phonon-mediated electron-electron attractions are responsible for the formation of Cooper pairs, whose condensation leads to the phenomena of conventional superconductivity [2]. Ultracold atoms have emerged as an ideal platform for engineering the interatomic interactions [3–5], testing the fundamental physics [6], and exploring the novel many-body quantum phenomena [7]. Of particular interest are the experimental observations of the fermion-mediated long-range interactions between bosons in Bose-Fermi mixtures in weakly interacting [8–10] and strongly interacting regimes [11,12]. This has sparked new interests in theoretical investigating of physics associated with the fermion-mediated interactions in various physical systems. These include studying the stability conditions for weakly interacting Bose-Fermi mixtures at zero temperature [13,14] and at finite temperatures [15], investigating mediated interactions with strong coupling theories [16,17] and effective field theories [18], and tailoring long-range interactions for quantum simulators [19].

Superfluid mixtures of bosonic and fermionic atoms have been the focus of both theoretical [20–28] and experimental [29–33] research over the past years. These double-superfluid systems provide fascinating opportunities to explore the interplay between excitations of distinct statistics and mediated interactions. A Bose-Fermi superfluid mixture possesses two gapless bosonic modes resulting from the spontaneous breaking of internal gauge symmetries of Bose superfluid and Fermi superfluid, respectively, and gapped fermionic excitations that describe the Cooper pair breaking [23,34,35]. One of the key questions to ask is how fermion-mediated interactions reshape our understanding of this exciting system. While existing experiments [29,33] on double-superfluid mixtures indicate damping of dipole modes, searching for well-defined quasiparticle excitations in interacting quantum matter represents one of the cornerstones of modern physics [36]. Superfluid mixtures of Bose-Fermi gases offer promising prospects to elucidate the physics of such quasiparticles.

In this work, we are trying to address this question by conducting the following studies: First, we start from the functional integral representation of the partition function of the system. By tracing out the fermions, we obtain an effective action entirely in terms of degrees of freedom associated with bosons, so that we can isolate the effects of fermion-mediated interactions on the bosons. Second, we examine how the induced interactions modify the Bogoliugov spectrum of bosons and lead to the damping of quasiparticles. Third, we map out the phase diagrams emphasizing the roles of the boson-fermion mass ratio and the boson-fermion interaction strength. Finally, by determining the behaviors of the tricritical point as a function of interfermion scattering length, we can completely characterize the topology of the phase diagram without recourse to extensive numerical treatment.

II. MODEL AND FORMALISM

We consider a homogeneous mixture of bosons and population balanced spin-1/2 fermions, described by the following

*ryliao@fjnu.edu.cn

grand canonical Hamiltonian:

$$H = \int d^3\mathbf{r}\Big[\sum_{\sigma=\uparrow,\downarrow}\psi_\sigma^\dagger(h_F + g_{BF}\phi^\dagger\phi)\psi_\sigma + g_F\psi_\uparrow^\dagger\psi_\downarrow^\dagger\psi_\downarrow\psi_\uparrow + \phi^\dagger h_B\phi + \frac{g_B}{2}\phi^\dagger\phi^\dagger\phi\phi\Big], \tag{1}$$

where $h_i = -\frac{\hbar^2}{2m_i}\nabla^2 - \mu_i$, $i = B$ or F denotes bosons or fermions with mass m_i, and μ_i represents the chemical potential. ϕ and ψ_σ are the field operators for bosons and fermions with spin $\sigma =\uparrow$ and $\downarrow$, respectively. In Bose gases, $g_B = 4\pi\hbar^2 a_B/m_B$, where positive s-wave scattering length a_B characterizes the repulsive interaction strength between bosons. In Fermi gases, g_F is the interaction strength between fermions and is assumed to be attractive, leading to Bardeen-Cooper-Schrieffer (BCS) pairing. $g_{BF} = 2\pi\hbar^2 a_{BF}(m_F^{-1} + m_B^{-1})$ accounts for the interaction strength between fermions and bosons, with a_{BF} being the corresponding s-wave scattering length. For convenience, we define the Fermi momentum $k_F = (3\pi^2 n_F)^{1/3}$, with n_F being the number density of Fermi gases, the Fermi velocity $v_F = \hbar k_F/m_F$, and the corresponding Fermi energy $E_F = \hbar^2 k_F^2/2m_F$. We adopt the natural units by setting $\hbar = k_B = 1$ for the sake of simplicity from now on.

Within the framework of the imaginary-time field integral [37], we can cast the partition function of the system as $\mathcal{Z} = \int \mathcal{D}[\bar\psi_\sigma, \psi_\sigma]\mathcal{D}[\phi^*, \phi]e^{-S}$, with the action given by $S = \int_0^\beta d\tau[H + \int d^3\mathbf{r}(\sum_\sigma \bar\psi_\sigma\partial_\tau\psi_\sigma + \phi^*\partial_\tau\phi)]$, where $\beta = 1/T$ is the inverse temperature. By performing a Hubbard-Stratonovich transformation, we introduce a bosonic field $\Delta(\mathbf{r}, \tau)$, which serves as an order parameter [38] encapsulating the relevant low-energy degrees of freedom for fermions. After carrying out the functional integration over the Grassmann fields, we can obtain an effective action $S_{\text{eff}} = \int d\tau d^3\mathbf{r}[\phi^*(\partial_\tau + h_B + \frac{g_B}{2}\phi^*\phi)\phi - |\Delta|^2/g_F] - \mathrm{Tr}\ln\mathcal{M} + \mathrm{Tr}\hat h$, with $\hat h = -\nabla^2/2m_F - \mu_F + g_{BF}\phi^*\phi$, where the matrix $\mathcal{M}$ reads

$$\mathcal{M} = \begin{pmatrix}\partial_\tau + \hat h & -\Delta \\ -\Delta^* & \partial_\tau - \hat h\end{pmatrix}. \tag{2}$$

So far, the above formal manipulation of the partition function is exact.

To facilitate the evaluation of the traces by benefiting the translational invariance, we transform the above to the momentum-frequency representation [$q \equiv (\mathbf{q}, \omega_n)$]. By making the Fourier expansions $\Delta = \Delta_0 + \sum_{q\neq 0}\Delta_q e^{iqx}$ (we set Δ_0 to be real) and $\phi^*\phi = \rho_0 + \sum_{q\neq 0}\rho_q e^{iqx}$ with space-time coordinate $x = (\mathbf{r}, \tau)$, and defining the inverse Green's function $\mathcal{G}^{-1} = -\partial_\tau + (\nabla^2/2m_F + \mu_F - g_{BF}\rho_0)\sigma_z + \Delta_0\sigma_x$, with σ_x and σ_z being the Pauli matrices, we can write $\mathcal{M} = -\mathcal{G}^{-1} + M_1$, where the matrix M_1 is

$$M_1 = \sum_{q\neq 0} e^{iqx}\begin{pmatrix} g_{BF}\rho_q & -\Delta_q \\ -\Delta_q^* & g_{BF}\rho_q\end{pmatrix}. \tag{3}$$

This allows one to write $\mathrm{Tr}\ln\mathcal{M} = \mathrm{Tr}\ln(-\mathcal{G}^{-1}) + \mathrm{Tr}\ln(I - \mathcal{G}M_1)$, with the unit matrix I, and to perform the series expansion $-\mathrm{Tr}\ln[I - \mathcal{G}M_1)] = \sum_l \mathrm{Tr}[(\mathcal{G}M_1)^l]/l$, with the positive integer l. For $l = 1$ and $l = 2$, we have

$$\mathrm{Tr}(\mathcal{G}M_1) = M_1(0)\sum_k \mathcal{G}(k) = 0, \tag{4a}$$

$$\mathrm{Tr}(\mathcal{G}M_1)^2 = \sum_{kq}\mathcal{G}(k)M_1(-q)\mathcal{G}(k+q)M_1(q). \tag{4b}$$

For $l \geqslant 3$, the related terms are usually related to the induced three-body or more than three-body interactions for bosons, which can be neglected for the dilute gases considered in this work. Therefore, up to the level of random-phase approximation, the effective action contains up to the quadratic order of the fluctuating fields Δ_q^* and Δ_q, which can be integrated out to yield an approximate effective action solely in terms of fields of Bose gases:

$$S_{\text{eff}} = \int d\tau d^3\mathbf{r}\phi^*\Big(\partial_\tau + h_B + \frac{g_B}{2}\phi^*\phi\Big)\phi + \frac{g_{BF}^2}{2}\sum_{q\neq 0}\Pi(q)\rho_{-q}\rho_q + \beta V\Big(\sum_{\mathbf{k}}\xi_{\mathbf{k}} - \frac{|\Delta_0|^2}{g_F}\Big) - \mathrm{Tr}\ln(-\mathcal{G}^{-1}) + \sum_q \ln\Gamma^{-1}(q), \tag{5}$$

where V represents the volume occupied by the system, and $S_{\text{NSR}} \equiv \sum_q \ln\Gamma^{-1}(q)$ is the so-called Nozieres–Schmitt-Rink (NSR) correction [39,40]. The extension of the original NSR theory to the superfluid phase below the transition temperature T_c has already been done by other researchers [41–48]. We have defined $\Pi(\mathbf{q}, z) = \Pi_{\text{pb}}(\mathbf{q}, z) + \Pi_{cl}(\mathbf{q}, z)$, where $\Pi_{cl} = -|\Delta_0|^2(I_{11}A^2 + z^2 I_{22}B^2 - 2z^2 I_{12}AB)/(I_{11}I_{22} - z^2 I_{12}^2)$ and $z = i\omega_n$ is the polarization function, describing the response of the superfluid Fermi gases under external density perturbation (ω_n is the bosonic Matsubara frequency). And $\Gamma^{-1}(q)$ and the parameters in the polarization function are given as follows:

$$A(\mathbf{q}, z) = \sum_{\mathbf{p}}\frac{E_+ + E_-}{E_+E_-}\frac{\xi_+ + \xi_-}{z^2 - (E_+ + E_-)^2}, \tag{6a}$$

$$B(\mathbf{q}, z) = \sum_{\mathbf{p}}\frac{E_+ + E_-}{E_+E_-}\frac{1}{z^2 - (E_+ + E_-)^2}, \tag{6b}$$

$$\Pi_{\text{pb}}(\mathbf{q}, z) = \sum_{\mathbf{p}}\frac{E_+ + E_-}{E_+E_-}\frac{E_+E_- - \xi_+\xi_- + |\Delta_0|^2}{z^2 - (E_+ + E_-)^2}, \tag{6c}$$

$$I_{11}(\mathbf{q}, z) = \sum_{\mathbf{p}}\frac{E_+ + E_-}{E_+E_-}\frac{E_+E_- + \xi_+\xi_- + |\Delta_0|^2}{z^2 - (E_+ + E_-)^2} + \frac{1}{E_{\mathbf{p}}}, \tag{6d}$$

$$I_{22}(\mathbf{q}, z) = \sum_{\mathbf{p}}\frac{E_+ + E_-}{E_+E_-}\frac{E_+E_- + \xi_+\xi_- - |\Delta_0|^2}{z^2 - (E_+ + E_-)^2} + \frac{1}{E_{\mathbf{p}}}, \tag{6e}$$

$$I_{12}(\mathbf{q}, z) = \sum_{\mathbf{p}}\frac{1}{E_+E_-}\frac{E_+\xi_- + E_-\xi_+}{z^2 - (E_+ + E_-)^2}, \tag{6f}$$

$$\Gamma^{-1}(\mathbf{q}, z) = I_{11}I_{22} - z^2 I_{12}^2, \tag{6g}$$

where $\pm$ is a shorthand notation for momentum $\mathbf{p} \pm \mathbf{q}/2$, $\xi_{\mathbf{p}} = \mathbf{p}^2/2m_F - \mu_F + g_{BF}|\phi_0|^2$, and $E_{\mathbf{p}} = \sqrt{\xi_{\mathbf{p}}^2 + |\Delta_0|^2}$. It is

interesting to notice that our approach recovers the same form of density-density correlation function $\Pi(\mathbf{q}, \omega + i0^+)$ obtained in studying collective modes with the dynamical BCS model formulated with a diagrammatic approach [49] and in studying dissipation of a moving impurity with time-dependent Bogoliugov-deGennes equations [50] in superfluid Fermi gases. It involves two contributions, one is from the pair-breaking excitations and the other is from the collective excitations.

We perform the standard Bogoliugov decomposition by writing $\phi = \phi_0 + \varphi$, where ϕ_0 and φ are the mean-field and fluctuating parts of the bosonic field, respectively. By retaining the fluctuating fields up to quadratic order, we approximate the effective action as $S_{\text{eff}} = S_0 + S_g + S_{\text{NSR}}$, where S_0 is the mean-field action and S_g is the Gaussian action containing the quadratic orders of φ and φ^*. Employing $\Omega = -\ln \mathcal{Z}/\beta V$, we obtain the grand potential density of the system at mean-field level as

$$\Omega^{(0)} = -\mu_B|\phi_0|^2 + \frac{g_B}{2}|\phi_0|^4 - \frac{|\Delta_0|^2}{g_F} + \frac{1}{V}\sum_{\mathbf{k}}(\xi_{\mathbf{k}} - E_{\mathbf{k}}) - \frac{2}{\beta V}\sum_{\mathbf{k}}\ln\left(1 + e^{-\beta E_{\mathbf{k}}}\right). \quad (7)$$

In principle, one should use the full grand potential Ω to determine the order parameters and the chemical potentials self-consistently, which will give quantitatively satisfactory results but it is numerically cumbersome. Here we undertake a compromise approach where quantum fluctuations are completely neglected but it is numerically tractable. We use the mean-field grand potential to determine equilibrium values of the order parameters and the chemical potentials, as it is self-consistent at mean-field level [51,52]. Effects of quantum fluctuations can be taken into account on top of the mean-field solutions [48,53,54]. Minimization of $\Omega^{(0)}$ with respect to Δ_0^* gives the gap equation $-1/g_F = (1/V)\sum_{\mathbf{k}} \tanh(\beta E_{\mathbf{k}}/2)/(2E_{\mathbf{k}})$. The thermodynamic relation $n_F = -\partial\Omega^{(0)}/\partial\mu_F$ gives the number equation $n_F = (1/V)\sum_{\mathbf{k}}[1 - \tanh(\beta E_{\mathbf{k}}/2)\xi_{\mathbf{k}}/E_{\mathbf{k}}]$. These two equations determine the order parameter $\Delta_0 = \Delta_0^c$ and the chemical potential $\mu_F = \mu_F^c + g_{BF}n_B$ self-consistently, where Δ_0^c and μ_F^c are the solutions in the absence of coupling with bosons, and n_B is the number density of Bose gases. The saddle-point condition $\partial\Omega^{(0)}/\partial\phi_0^* = 0$ leads to the Hugenholz-Pines theorem [55], yielding the relation $\mu_B = g_B n_B + g_{BF}n_F$. At zero temperature, the corresponding ground-state energy density is found from the relation $E_G^{(0)} = \Omega^{(0)} + \mu_F n_F + \mu_B n_B$, yielding

$$E_G^{(0)} = \alpha n_F E_F + \frac{g_B}{2}n_B^2 + g_{BF}n_F n_B, \quad (8a)$$

$$\alpha(\eta) = \frac{\mu_F^c}{E_F} - \frac{3\pi}{8k_F a}\frac{|\Delta_0|^2}{E_F^2} + \frac{1}{n_F E_F V}\sum_{\mathbf{k}}\left(\xi_{\mathbf{k}} + \frac{|\Delta_0|^2}{2\epsilon_{\mathbf{k}}} - E_{\mathbf{k}}\right). \quad (8b)$$

In the above, we have expressed the bare coupling parameter g_F in favor of the physical scattering length a via the prescription $1/g_F = m_F/(4\pi a) - (1/V)\sum_{\mathbf{k}} 1/(2\epsilon_{\mathbf{k}})$, with $\epsilon_{\mathbf{k}} = \mathbf{k}^2/(2m_F)$. As seen above, the dimensionless coefficient $\alpha(\eta)$ is fully determined by the coupling parameter $\eta \equiv 1/(k_F a)$. Typically, in the deep BCS limit, we have α approaching 3/5, recovering the well-known result for free fermions [13,56].

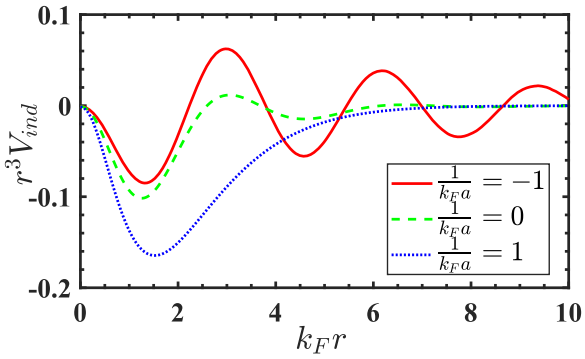

FIG. 1. The spatial distribution of r^3 scaling of the induced interaction potential $r^3V_{\text{ind}}(r)$ [in units of $g_{BF}^2 d(E_F)$] between two bosons with the relative coordinate $\mathbf{r}$ for three typical interaction parameters $k_F a = -1$, 0, and 1, corresponding respectively to the regions of BCS, unitarity, and BEC. $d(E_F) = m_F k_F/\pi^2$ is the density of states of free Fermi gases at the Fermi energy.

To ensure the stability of the system, we require that the Hessian matrix $\partial^2 E_G^{(0)}/\partial n_i \partial n_j$ with $i, j = F, B$ constructed for the ground state to be positive definite, which leads to an upper bound for fermion density of

$$n_F^{1/3} < \frac{5(3\pi^2)^{2/3} g_B}{9 m_F g_{BF}^2}\left[\alpha - \frac{3}{5}\eta\frac{\partial\alpha}{\partial\eta} + \frac{1}{10}\eta^2\frac{\partial^2\alpha}{\partial\eta^2}\right], \quad (9)$$

which is a generalization of the mechanical stability condition for Bose-Fermi mixtures [56]. Noticing that the sound velocity of the BCS system can be determined via $v_s^2 = (n_F/m_F)\partial^2 E_G^{(0)}/\partial n_F^2$, we obtain an equivalent stability condition for the system against phase separation as $n_F < v_s^2 m_F g_B/g_{BF}^2$, which has been checked consistently in numerics.

III. RESULTS AND DISCUSSION

Inspecting the effective action in Eq. (5) and the polarization function, one can obtain the Hamiltonian describing the induced two-body interactions between bosons through coupling with fermions, that is, $H_{\text{ind}} = (g_{BF}^2/2)\sum_{\mathbf{q}\neq 0}\sum_{\mathbf{k},\mathbf{p}} \Pi_{\mathbf{q}} \phi_{\mathbf{k}+\mathbf{q}}^\dagger \phi_{\mathbf{p}-\mathbf{q}}^\dagger \phi_{\mathbf{p}}\phi_{\mathbf{k}}$, where $\Pi_{\mathbf{q}} \equiv \Pi(\mathbf{q}, 0)$ is the polarization function evaluated at the static limit at zero temperature. Correspondingly, an induced pairwise interaction potential between two Bose atoms with the relative coordinate $\mathbf{r}$ is given by $V_{\text{ind}}(\mathbf{r}) = \sum_{\mathbf{q}\neq\mathbf{0}} g_{BF}^2 \Pi_{\mathbf{q}} e^{i\mathbf{q}\cdot\mathbf{r}}$. The r^3 scaling behavior of the induced potential $r^3 V_{\text{ind}}$ is presented in Fig. 1. The essential features of the fermion-mediated interaction potential are remarkable: On the BCS side with $1/k_F a = -1$, the potential shows an oscillating power-law behavior $(1/r^3)$, a signature of the oscillatory Ruderman-Kittel-Kasuya-Yosida (RKKY) type interaction [57]. The RKKY interaction originally describes the effective interaction between two localized magnetic impurities due to the polarization of the conduction electrons near the Fermi surface. For Bose-Fermi mixtures, the effective interaction

potential between bosons mediated by a single species fermions is predicted [58–60] to be of RKKY type in real space, where it decays at $1/r^3$ at large spatial separation and shows the Friedel oscillations at a period of $1/2k_F$, imprinted by the density of the Fermi gases. At unitary with $1/k_F a = 0$, the potential still shows power-law behavior, but with small range. On the Bose-Einstein condensation (BEC) side with $1/k_F a = 1$, the potential decreases to zero rather quickly as expected, as at the BEC limit it has been shown to induce an attractive Yukawa potential ($e^{-\sqrt{2}r/\xi}/r$) that falls off exponentially beyond the healing length ξ [61–63].

The Gaussian action for the bosonic fluctuating fields can be compactly written as $S_g = \frac{1}{2}\sum_q \Phi_q^\dagger \mathcal{G}_B^{-1}\Phi_q$ by defining a column vector $\Phi_q = (\varphi_q, \varphi_{-q}^*)^T$ and an inverse matrix $\mathcal{G}_B^{-1} = \epsilon_q + A_q - i\omega_n\sigma_z + A_q\sigma_x$, with $\epsilon_{\mathbf{q}} = \mathbf{q}^2/2m_B$ and $A_q = (g_{BB} + g_{BF}^2\Pi_q)n_B$. The quasiparticle spectrum $\omega(\mathbf{q})$ and the damping rate $\gamma(\mathbf{q})$ can be obtained by seeking solutions of the secular equation $det\mathcal{G}_B^{-1}(\mathbf{q}, \omega - i\gamma) = 0$ with substitution of $\Pi_q|i\omega_n \to \omega + i0^\dagger$. By analytic continuation to real frequency ($i\omega_n \to \omega + i0^\dagger$), one obtains the polarization function $\Pi(\mathbf{q}, \omega)$, whose imaginary part provides essential information for the damping of the excitations of Bose gases. The imaginary part of the polarization is closely related to the pole of Π, which corresponds to the excitation spectrum of the superfluid Fermi gases.

In Fig. 2(a), we show two types of excitation at the unitary limit, where both pair-breaking excitation and collective excitation are important. The pair-breaking excitation spectrum $\omega_{\rm pb}$ corresponds to the poles of $\Pi_{\rm pb}(\mathbf{q}, z)$, namely, $\omega_{\rm pb} = E_+ + E_-$. It is a single-particle continuum, and its minimum $\omega_{\rm th}(\mathbf{q})$ denotes the threshold energy to break a Cooper pair with center-of-mass momentum $\mathbf{q}$. The shaded region denotes that the imaginary part of the polarization differs from zero and is referred to as the pair-breaking continuum. The collective spectrum $\omega_{\rm col}(\mathbf{q})$ can be found by seeking the poles of $\Pi_{\rm cl}(\mathbf{q}, z)$, yielding $I_{11}(\mathbf{q}, \omega)I_{22}(\mathbf{q}, \omega) - \omega^2 I_{12}^2(\mathbf{q}, \omega) = 0$. The collective excitation spectrum exhibits characteristic linear energy-momentum behavior at small momentum q as it is a sound mode, and it lies below the pair-breaking threshold. The behaviors of the imaginary part of the polarization function for three typical momenta $q/k_F = 1.0$, 1.5, and 2.0 are shown in Fig. 2(b). For $q/k_F = 1.0$ and 1.5, they have the same threshold energy $2\Delta_0$, below which $\mathrm{Im}\Pi(q, \omega)$ vanishes, while for $q/k_F = 2.0 > 4\mu_F^c$, the threshold energy is given by $\omega_{\rm th} = \sqrt{(q^2/4 - \mu^c)^2 + \Delta_0^2}$. The magnitude of $\mathrm{Im}\Pi(q, \omega)$ reaches maximum right after the threshold energy and decreases quickly with increasing energy.

The behaviors of the Bogoliubov spectrum $\omega(q)$ and the damping rate $\gamma(q)$ for three typical mass ratios $r_m = m_B/m_F$ are shown in Figs. 2(c) and 2(d). At small momentum, the spectrum is phononlike with the sound velocity given by $c = \sqrt{(g_B + g_{BF}^2\Pi_0)n_B/m_B}$. For $r_m = 1$, as shown in Fig. 2(c), there is a cusp in the spectrum resulting from the avoid-crossing of collective modes of the Fermi superfluid and the Bose superfluid. For sufficiently large momentum q, both spectrums for $r_m = 1$ and $r_m = 1.5$ are entering the pair-breaking continuum, signifying that the Bogoliubov quasiparticle achieves finite lifetime due to damping effects. The damping occurs when the quasiparticle energy reaches

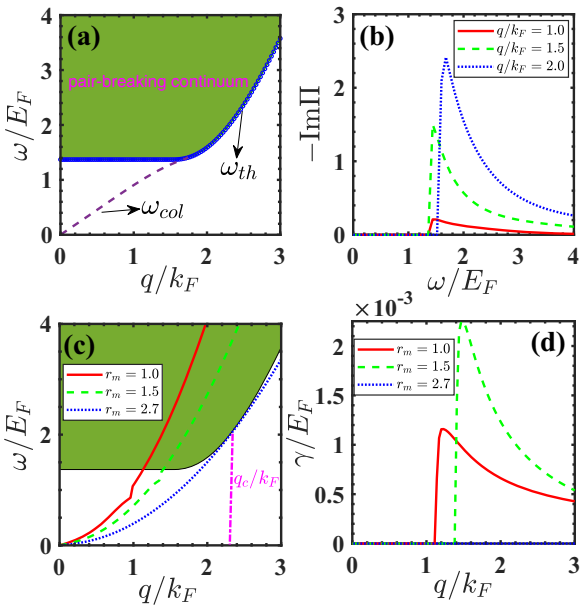

FIG. 2. Physics of excitations and damping at the unitarity where $1/k_F a = 0$. Shown in the upper panels are properties of the polarization function. (a) The shaded region is the range where the imaginary part of the polarization differs from zero and is referred as the pair-breaking continuum. $\omega_{\rm th}$ denotes the threshold for the pair-breaking excitation, and $\omega_{\rm col}$ is the collective excitation. (b) The imaginary part of the polarization function $\mathrm{Im}\Pi(\mathbf{q}, \omega)$ [in units of $d(E_F)$] as a function of frequency ω for given typical momentum amplitudes q. Shown in the lower panels are properties of the Bogoliubov quasiparticles. (c) The excitation energy ω/E_F and (d) the Landau damping rate γ/E_F for three typical mass ratios: $r_m = 1.0$, 1.5, and 2.7. $d(E_F) = m_F k_F/\pi^2$ is the density of states of free Fermi gases at the Fermi energy. The relevant parameters chosen here are $k_F a_B = 0.1$, $k_F a_{BF} = 0.05$, and $n_B/n_F = 1$.

the threshold energy $\omega_{\rm th}$, swiftly reaches its maximum, and decreases gradually for increasing momentum. Remarkably, there exists a critical mass ratio $r_m = 2.7$, above which Bogoliugov excitations can achieve infinite lifetime with no damping. This special line of spectrum for $r_m = 2.7$ intercepts the curve of the threshold energy at a critical momentum, q_c, and the damping vanishes for arbitrary momentum, as shown in Fig. 2(d).

We are now in position to construct a phase diagram for the system. The stability constraint marks the transition line between stable phase mixing and phase separation (PS) into fermions and bosons [25,56,64,65], which remains the same for different number density ratios n_B/n_F, as shown in Figs. 3 and 4, corresponding to $1/k_F a = -1$ (BCS side) and $1/k_F a = 0$ (unitarity limit), respectively. In the stable-phase-mixing region, we can further classify it into regions accommodating quasiparticle excitations with and without damping, termed as damped and QP, respectively. To map out the phase boundary separating the damped region and the QP region, one needs to require that at the phase boundary the quasiparticle spectrum $\omega(q)$ is the tangent line to the threshold energy $\omega_{\rm th}(q)$, which simultaneously determines both the critical momentum q_c and the critical mass ratio r_m, illustrated previously in Fig. 2(c).

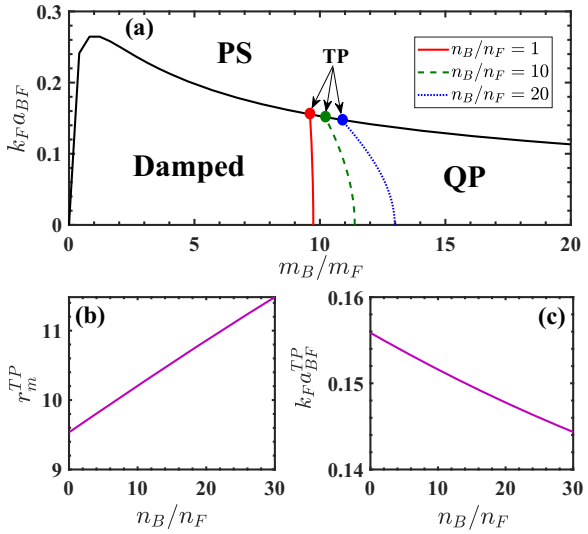

FIG. 3. (a) Phase diagram spanned by the boson-fermion mass ratio and the coupling strength $k_F a_{BF}$ at $1/k_F a_{FF} = -1$ (BCS side). It has three regions: phase separation (PS), quasiparticle with infinite lifetime (QP), and a damped region where the quasiparticle has finite lifetime due to damping. For the given boson-fermion density ratio, the three regions meet at a tricritical point (TP). (a), (b) The evolution of the tricritical point ($r_m^{\rm TP}$, $k_F a_{BF}^{\rm TP}$) as a function of the boson-fermion density ratio n_B/n_F.

At the BCS side with $1/k_F a = -1$, as shown in Fig. 3(a), the largest boson-fermion coupling strength $k_F a_{FB}$ one can achieve to sustain a homogenous phase increases sharply, reaches a peak with $k_F a_{FB} = 0.27$ at $m_B/m_F = 1$, and decreases slowly with increasing boson-fermion mass ratio r_m.

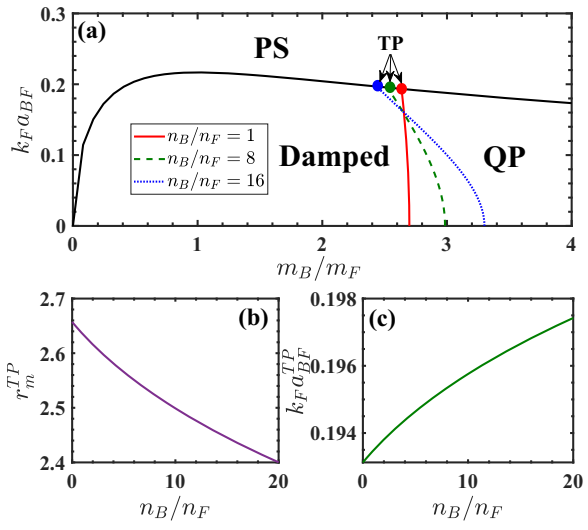

FIG. 4. (a) Phase diagram spanned by the mass ratio and the boson-fermion coupling strength $k_F a_{BF}$ at $1/k_F a_{FF} = 0$ (unitarity). It has three regions: phase separation (PS), quasiparticle with infinite lifetime (QP), and a damped region where the quasiparticle has finite lifetime due to damping. For the given boson-fermion density ratio, the three regions meet at a tricritical point (TP). (a, b) The evolution of the tricritical point ($r_m^{\rm TP}$, $k_F a_{BF}^{\rm TP}$) as a function of boson-fermion density ratio n_B/n_F.

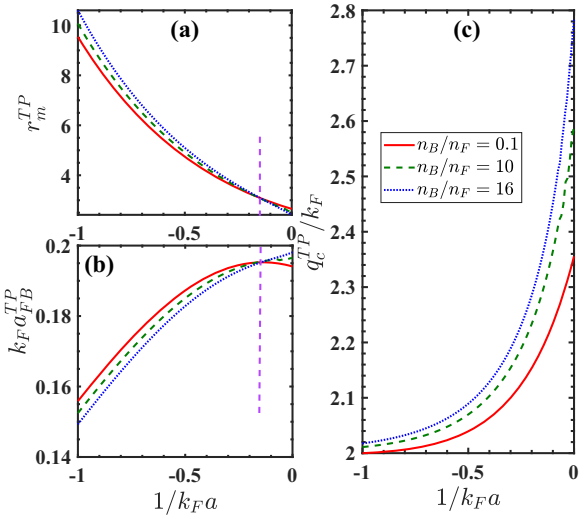

FIG. 5. (a), (b) Evolution of the TP ($r_m^{\rm TP}$, $k_F a_{BF}^{\rm TP}$) as a function of $1/k_F a$. (c) Evolution of the critical momentum $q_c^{\rm TP}$ at the TP as a function of $1/k_F a$.

As the boson-fermion density ratio n_B/n_F increases, the regime of QP diminishes, giving way to the damped region. The tricritical point (TP) ($r_m^{\rm TP}$, $k_F a_{FB}^{\rm TP}$) where the three phases meet can be tuned to move with the density ratio n_B/n_F, as shown in Figs. 3(a) and 3(b). The tricritical point moves toward a high boson-fermion mass ratio and a low boson-fermion coupling strength when n_B/n_F increases.

At the unitarity limit where $1/k_F a = 0$, as shown in Fig. 4(a), the phase boundary line between the phase mixing and the phase separation varies smoothly with increasing boson-fermion mass ratio m_B/m_F. The phase diagram accommodates large portions of the QP region, as the boundary for the boson-fermion mass ratio could reach $m_B/m_F = 2.65$ when $n_B/n_F \to 0$. As n_B/n_F increases, the TP moves toward a low mass ratio r_m and a high boson-fermion coupling strength $k_F a_{BF}$, in stark contrast to the case of $1/k_F a = -1$.

How the interaction parameter $1/k_F a$ controls the motion of the tricritical point becomes an interesting thing to investigate. This is shown in Fig. 5. For all three typical density ratios $n_B/n_F = 0.1$, 8, and 16, the critical mass ratio $r_m^{\rm TP}$ decreases as one tunes up the BCS coupling strength $1/k_F a$, as seen in Fig. 5(a). Conversely, the critical boson-fermion coupling strength $k_F a_{BF}$ increases as one ramps up the BCS coupling strength $1/k_F a$, as seen in Fig. 5(b). What is striking is that the behavior of the TP as a function of the density ratio n_B/n_F shows a reverse trend when it touches a critical BCS coupling strength roughly at $1/k_F a = -0.16$. However, the critical momentum $q_c^{\rm TP}$ follows the same trends for both the BCS coupling strength and the density ratio, as evident in Fig. 5(c).

IV. CONCLUSIONS

In summary, we have investigated the superfluid mixtures of bosonic and fermionic atoms. By using the functional integral method to trace out the fermionic degrees of freedom, the effective action of the system shows that the induced interactions mediated by fermions between bosons are attractive

interactions, and it shows long-range behavior in the BCS regime that gradually becomes short-ranged when it is driven toward the BEC limit. By analyzing the Bogoliubov spectrum and the damping rate of bosonic superfluid, we have mapped out the phase diagram in the parameter space spanned by the boson-fermion mass ratio and the boson-fermion coupling strength, which shows that the stable-phase-mixing region can be further classified by damping of excitations, leading to a tricritical point in the phase diagram. A series of new features arising from fermion-mediated interactions have also been identified. The predicted damping rate can be probed experimentally via two-phonon Bragg spectroscopy [66]. Experimental verification of the predicted phase diagram will constitute an important step along the lines of searching for well-defined quasiparticle excitations in these systems. We hope that our work can add new excitement to the surging field of cold-atom physics involving fermion-mediated interactions.

ACKNOWLEDGMENTS

R.L. acknowledges funding from the NSFC under Grants No.12174055 and No.11674058 and by the Natural Science Foundation of Fujian under Grant No. 2020J01195. L.W. acknowledges the funding from the NSFC under Grant No. 12175027.

[1] S. Weinberg, *The Quantum Theory of Fields* (Cambridge University, Cambridge, England, 1995).
[2] S. M. Girvin and K. Yang, *Modern Condensed Matter Physics* (Cambridge University, Cambridge, England, 2019).
[3] C. Chin, R. Grimm, P. Julienne, and E. Tiesinga, Feshbach resonances in ultracold gases, Rev. Mod. Phys. **82**, 1225 (2010).
[4] H. Ritsch, P. Domokos, F. Brennecke, and T. Esslinger, Cold atoms in cavity-generated dynamical optical potentials, Rev. Mod. Phys. **85**, 553 (2013).
[5] J. Dalibard, F. Gerbier, G. Juzeliunas, and P. Öhberg, Colloquium: Artifical gauge potentials for neutral atoms, Rev. Mod. Phys. **83**, 1523 (2011).
[6] I. M. Georgescu, S. Ashhab, and F. Nori, Quantum simulation, Rev. Mod. Phys. **86**, 153 (2014).
[7] I. Bloch, J. Dalibard, and W. Zwerger, Many-body physics with ultracold gases, Rev. Mod. Phys. **80**, 885 (2008).
[8] B. J. DeSalvo, K. Patel, G. Cai, and C. Chin, Observation of fermion-mediated interations between bosonic atoms, Nature (London) **568**, 61 (2019).
[9] G. M. Bruun, New interactions seen in an ultracold gas, Nature (London) **568**, 37 (2019).
[10] H. Edri, B. Raz, N. Matzliah, N. Davidson, and R. Ozeri, Observation of spin-spin fermion-mediated interactions between ultracold atoms, Phys. Rev. Lett. **124**, 163401 (2020).
[11] K. Patel, G. Cai, H. Ando, and C. Chin, Sound propagation in a Bose-Fermi mixture: From weak to strong interactions, Phys. Rev. Lett. **131**, 083003 (2023).
[12] X.-Y. Chen, M. Duda, A. Schindewolf, R. Bause, I. Bloch, and X.-Y. Luo, Supression of unitary three-body loss in a degenerate Bose-Fermi mixture, Phys. Rev. Lett. **128**, 153401 (2022).
[13] D.-C. Zheng, C.-R. Ye, L. Wen, and R. Liao, Polarizing the medium: Fermion-mediated interactions between bosons, Phys. Rev. A **103**, L021301 (2021).
[14] R. Liao, Ultracold bose mixtures with spin-dependent fermion-mediated interactions, Phys. Rev. Res. **2**, 043218 (2020).
[15] K. Manabe and Y. Ohashi, Thermodynamic stability, compressibility matrices, and effects of mediated interactions in a strongly interacting Bose-Fermi mixture, Phys. Rev. A **103**, 063317 (2021).
[16] S. Ding, M. Drewsen, J. J. Arlt, and G. M. Bruun, Mediated interactions between ions in quantum degenerate gases, Phys. Rev. Lett. **129**, 153401 (2022).
[17] Q.-D. Jiang, On the sign of fermion-mediated interactions, Phys. Rev. B **103**, L121107 (2021).
[18] K. Fujii, M. Hongo, and T. Enss, Universal van der Waals force between heavy polarons in superfluids, Phys. Rev. Lett. **129**, 233401 (2022).
[19] J. Argüello-Luengo, A. González-Tudela, and D. González-Cuadra, Tuning long-range fermion-mediated interactions in cold-atom quantum simulators, Phys. Rev. Lett. **129**, 083401 (2022).
[20] B. Ramachandhran, S. G. Bhongale, and H. Pu, Finite-temperature study of Bose-Fermi superfluid mixtures, Phys. Rev. A **83**, 033607 (2011).
[21] T. Ozawa, A. Recati, M. Delehaye, F. Chevy, and S. Stringari, Chandrasekhar-Clogston limit and critical polarization in a Fermi-Bose superfluid mixture, Phys. Rev. A **90**, 043608 (2014).
[22] W. Zheng and H. Zhai, Quasiparticle lifetime in a mixture of Bose and Fermi superfluids, Phys. Rev. Lett. **113**, 265304 (2014).
[23] R. Zhang, W. Zhang, H. Zhai, and P. Zhang, Calibration of the interaction energy between Bose and Fermi superfluids, Phys. Rev. A **90**, 063614 (2014).
[24] J. J. Kinnunen and G. M. Bruun, Induced interactions in a superfluid Bose-Fermi mixture, Phys. Rev. A **91**, 041605(R) (2015).
[25] M. Tylutki, A. Recati, F. Dalfovo, and S. Stringari, Dark-bright solitons in a superfluid Bose-Fermi mixture, New J. Phys. **18**, 053014 (2016).
[26] Y. Jiang, R. Qi, Z.-Y. Shi, and H. Zhai, Vortex lattices in the Bose-Fermi superfluid mixture, Phys. Rev. Lett. **118**, 080403 (2017).
[27] F. K. Abdullaev, M. Ögren, and M. P. Sørensen, Collective dynamics of Fermi-Bose mixtures with an oscillating scattering length, Phys. Rev. A **99**, 033614 (2019).
[28] M. Ögren and G. M. Kavoulakis, Rotational properties of superfluid Fermi-Bose mixtures in a tight toroidal trap, Phys. Rev. A **102**, 013323 (2020).
[29] I. Ferrier-Barbut, M. Delehaye, S. Laurent, A. T. Grier, M. Pierce, B. S. Rem, F. Chevy, and C. Salomon, A mixture of Bose and Fermi superfluids, Science **345**, 1035 (2014).
[30] M. Delehaye, S. Laurent, I. Ferrier-Barbut, S. Jin, F. Chevy, and C. Salomon, Critical velocity and dissipation of an ultracold Bose-Fermi counterflow, Phys. Rev. Lett. **115**, 265303 (2015).

[31] X.-C. Yao, H.-Z. Chen, Y.-P. Wu, X.-P. Liu, X.-Q. Wang, X. Jiang, Y. Deng, Y.-A. Chen, and J.-W. Pan, Observation of coupled vortex lattices in a mass-imbalance Bose and Fermi superfluid mixture, Phys. Rev. Lett. **117**, 145301 (2016).

[32] R. Roy, A. Green, R. Bowler, and S. Gupta, Two-element mixture of Bose and Fermi superfluids, Phys. Rev. Lett. **118**, 055301 (2017).

[33] Y.-P. Wu, X.-C. Yao, X.-P. Liu, X.-Q. Wang, Y.-X. Wang, H.-Z. Chen, Y. Deng, Y.-A. Chen, and J.-W. Pan, Coupled dipole oscillations of a mass-imbalanced Bose-Fermi superfluid mixture, Phys. Rev. B **97**, 020506(R) (2018).

[34] S. Hoinka, P. Dyke, M. G. Lingham, J. K. Kunnunen, G. M. Bruun, and C. J. Vale, Goldstone mode and pair-breaking excitations in atomic Fermi superfluids, Nat. Phys. **13**, 943 (2017).

[35] S. Klimin, J. Tempere, T. Repplinger, and H. Kurkjian, Collective excitations of a charged Fermi superfluid in the BCS-BEC crossover, New J. Phys. **25**, 063011 (2023).

[36] Z. Z. Yan, Y. Ni, C. Robens, and M. W. Zwielein, Bose polarons near quantum criticality, Science **368**, 190 (2020).

[37] A. Altland and B. Simions, *Condensed Matter Field Theory*, 2nd ed. (Cambridge University, Cambridge, England, 2010).

[38] The superflid order parameter can be determined self-consistently as $\Delta(\mathbf{r},\tau) = -g_F\langle\psi_\downarrow(\mathbf{r},\tau)\psi_\uparrow(\mathbf{r},\tau)\rangle$ by imposing the saddle-point condition $\delta S/\delta\Delta(\mathbf{r},\tau) = 0$.

[39] P. Nozieŕes and S. Schmitt-Rink, Bose condensation in an attractive fermion gas: From weak to strong coupling superconductivity, J. Low Temp. Phys. **59**, 195 (1985).

[40] C. A. R. Sá de Melo, M. Randeria, and J. R. Engelbrecht, Crossover from BCS to Bose superconductivity: Transition temperature and time-dependent Ginzburg-Landau theory, Phys. Rev. Lett. **71**, 3202 (1993).

[41] R. Haussmann, Properties of a Fermi liquid at the superfluid transition in the crossover region between BCS superconductivity and Bose-Einstein condensation, Phys. Rev. B **49**, 12975 (1994).

[42] J. R. Engelbrecht, M. Randeria, and C. A. R. Sáde Melo, BCS to Bose crossover: Broken-symmetry state, Phys. Rev. B **55**, 15153 (1997).

[43] Q. Chen, J. Stajic, S. Tan, and K. Levin, BCS-BEC crossover: From high temperature superconductors to ultracold superfluids, Phys. Rep. **412**, 1 (2005).

[44] A. Perali, P. Pieri, and G. C. Strinati, Quantitative comparison between theoretical predictions and experimental results for the BCS-BEC crossover, Phys. Rev. Lett. **93**, 100404 (2004).

[45] H. Hu, X.-J. Liu, and P. D. Drummond, Equation of state of a superfluid Fermi gas in the BCS-BEC crossover, Europhys. Lett. **74**, 574 (2006).

[46] H. Hu, P. D. Drummond, and X.-J. Liu, Universal thermodynamics of strongly interacting Fermi gases, Nat. Phys. **3**, 469 (2007).

[47] R. Haussmann, W. Rantner, S. Cerrito, and W. Zwerger, Thermodynamics of the BCS-BEC crossover, Phys. Rev. A **75**, 023610 (2007).

[48] R. B. Diener, R. Sensarma, and M. Randeria, Quantum fluctuations in the superfluid state of the BCS-BEC crossover, Phys. Rev. A **77**, 023626 (2008).

[49] R. Combescot, M. Y. Kagan, and S. Stringari, Collective mode of homogeneous superfluid Fermi gases in the BEC-BCS crossover, Phys. Rev. A **74**, 042717 (2006).

[50] D.-C. Zheng, Y.-Q. Yu, and R. Liao, Tuning dissipation and excitations in superfluid Fermi gases with a moving impurity, Phys. Rev. A **100**, 033611 (2019).

[51] D. E. Sheehy and L. Radzihovsky, BEC-BCS crossover in "magnetized" Feshbach-resonantly paired superfluids, Phys. Rev. Lett. **96**, 060401 (2006).

[52] R. Liao and K. F. Quader, Pairing in asymmetrical Fermi systems with intra- and interspecies correlations, Phys. Rev. B **76**, 212502 (2007).

[53] M. Randeria and E. Taylor, Crossover from Bardeen-Cooper-Schrieffer to Bose-Einstein condensation and the unitary Fermi gas, Annu. Rev. Condens. Matter Phys. **5**, 209 (2014).

[54] L. He, Dynamic density and spin responses of a superfluid Fermi gas in the BCS-BEC crossover: Path integral formulation and pair fluctuation theory, Ann. Phys. **373**, 470 (2016).

[55] N. Hugenholz and D. Pines, Ground-state energy and excitation spectrum of a system of interacting bosons, Phys. Rev. **116**, 489 (1959).

[56] L. Viverit, C. J. Pethick, and H. Smith, Zero-temperature phase diagram of binary boson-fermion mixtures, Phys. Rev. A **61**, 053605 (2000).

[57] M. A. Ruderman and C. Kittel, Indirect exchange coupling of nuclear magnetic moments by conduction electrons, Phys. Rev. **96**, 99 (1954).

[58] D. H. Santamore and E. Timmermans, Fermion-mediated interactions in a dilute Bose-Einstein condensate, Phys. Rev. A **78**, 013619 (2008).

[59] S. De and I. B. Spielman, Fermion-mediated long-range interactions between bosons stored in an optical lattice, Appl. Phys. B **114**, 527 (2014).

[60] D. Suchet, Z. Wu, F. Chevy, and G. M. Bruun, Long-range mediated interactions in a mixed-dimensional system, Phys. Rev. A **95**, 043643 (2017).

[61] E. Nakano and H. Yabu, BEC-polaron gas in a boson-fermion mixture: A many-body extention of Lee-Low-Pines theory, Phys. Rev. B **93**, 205144 (2016).

[62] A. Camacho-Guardian, L. A. Peña Ardila, T. Pohl, and G. M. Bruun, Bipolarons in a Bose-Einstein condensate, Phys. Rev. Lett. **121**, 013401 (2018).

[63] A. Camacho-Guardian and G. M. Bruun, Landau effective interaction between quasiparticles in a Bose-Einstein condensate, Phys. Rev. X **8**, 031042 (2018).

[64] K. Mølmer, Bose condensates and Fermi gases at zero temperature, Phys. Rev. Lett. **80**, 1804 (1998).

[65] R. Roth, Structure and stability of trapped atomic boson-fermion mixtures, Phys. Rev. A **66**, 013614 (2002).

[66] R. Ozeri, N. Katz, J. Steinhauer, and N. Davidson, Colloquium: Bulk Bogoliubov excitations in a Bose-Einstein condensate, Rev. Mod. Phys. **77**, 187 (2005).